Deposition of MgO Nanoparticles by Laser Pyrolysis

Hala M. Abdulwahab[1], Bassam G. Rasheed[2], Hanadi H. Altawil[3]

Authors affiliations:

1) Laser and Optoelectronics Eng. Dept., Al-Nahrain University, Baghdad-Iraq.
st.hala.m.abdulwahab@ced.nahrainuniv.edu.iq

2*) Laser and Optoelectronics Eng. Dept., Al-Nahrain University, Baghdad-Iraq.
bassam.g.rasheed@nahrainuniv.edu.iq

3)Mathematics, Computer & Natural Sciences Division of Ohio Dominican University, USA
altawilh@ohiodominican.edu

Abstract

Magnesium oxide nanoparticles were deposited by laser pyrolysis process. Three types of lasers were employed CW CO_2, Q-switched Nd-YAG (short pulses) and long pulses Nd-YAG lasers. The size and density of nanoparticles vary with laser energy, power, pulse duration and the scanning speed of the laser. In this method, MgO nanoparticles were deposited by a laser beam on a quartz substrate from aqueous solution of magnesium nitrate. AFM images reveal formation of small nanoparticle size of 24.5 nm with surface roughness 6.97nm by Q-switched Nd-YAG laser (10 ns) when the energy was 1J. While for CO_2 laser, the smallest size was 18.8 nm at 0.4mm/s scanning speed with surface roughness 5.21nm at the same scanning speed. Moreover, long Nd-YAG pulses laser produces relatively larger average size of 37.5nm at 0.8ms pulse duration. The absorption spectra from UV-Visible spectroscopy were also conducted. The best absorption intensity was obtained at a wavelength ranging between 420-430 nm for both lasers. Finally, Thermal analysis using COMSOL Multiphysics software for the deposition process reveals that maximum temperature about 440Kfor Q-Switched Nd-YAG laser at 1J laser energy. While for RF CO_2 laser, the maximum temperature obtained at 0.4mm/s scanning speed is 850K.This work provides a good knowledge for the deposition of nanoparticles using laser beams.

Keywords: MgO Nanoparticles, Laser Pyrolysis, Nanoparticles Deposition.

ترسب جسيمات اوكسيد المغنيسيوم النانوية بواسطة الانحلال الحراري بالليزر

هاله محمودعبدالوهاب، بسام غالب رشيد، هنادي هادي الطويل

الخلاصة:

تم ترسيب جزيئات أكسيد المغنيسيوم النانوية بواسطة عملية الانحلال الحراري بالليزر.استخدم ثلاثة أنواع من الليزر ليزر CO_2 CW وليزرQ-switched Nd-YAG ذوالنبضات القصيرة وأشعة الليزر Nd-YAG ذو النبضات الطويلة. وجد بانه حجم وكثافة الجسيمات النانوية باختلاف طاقة الليزر والطاقة وامدنبضة الليزر وسرعة مسح الليزر. في هذه الطريقة ، جزيئات MgO النانوية بواسطة شعاع ليزر على ركيزة كوارتز من محلول مائي من نترات المغنيسيوم. تكشف صور AFM عن تكوين حجم جسيم نانوي صغير يبلغ ٢٤,٥ نانومتر مع خشونة السطح ٦,٩٧ نانومتر بواسطة ليزر Q-switched Nd-YAG (١٠ نانوثانية) عندما كانت الطاقة ١جول .بينا بالنسبة للبزر ثاني أكسيد الكربون ،كان أصغر حجم ١٨,٨ نانومتر بسرعة مسح ٠,٤ م/ثانية مع خشونة السطح ٥,٢١ نانومتر بنفس سرعة المسح. علاوة على ذلك ، ينتج ليزر النبضات الطويلة Nd-YAG حجم دقائق نانوية متوسط أكبرنسبيًا يبلغ ٣٧,٥ نانومترعند مدة نبضة تبلغ ٠,٨ مللي ثانية.أجريت أطياف الامتصاص من التحليل الطيفي للأشعة فوق البنفسجية المرئية. حيث تم الحصول على أفضل كثافة امتصاص عند طول موجي يتراوح بين ٤٢٠-٤٣٠ نانومتر لكلاالليزرين. أخيرًا ، يكشف التحليل الحراري باستخدام برنامج COMSOL لعملية الترسيب أن درجة الحرارة القصوى كانت حوالي ٤٤٠ كلفن للبزر Q-Switched Nd-YAG عند طاقة ليزر ١ جول بينا بالنسبة إلى ليزر ثاني أكسيد الكربون RF ، فإن أقصى درجة حرارة تم الحصول عليها عند سرعة المسح ٠,٤ م/ثانية كانت ٨٥٠ كلفن. هذا العمل يوفر معرفة جيدة لترسب الجسيمات النانوية باستخدام أشعة الليزر.

1. Introduction

Nanoparticles of magnesium oxide is considered as an attractive material due to its characteristics that make it useful for wide range of applications, such as optoelectronics, paint, water purification, microelectronics circuit, chemical sensors, bactericides and gas sensors. Magnesium oxide has distinctive and unique electronic, optical, mechanical, thermal, magnetic and chemical properties [1, 2]. Laser pyrolysis is a unique technology that can be employed to synthesize nanomaterials and thin films [3]. This technique involves absorption of laser beam by the substrate and subsequently deposit the required nanomaterial [4].

In this process, chemical compound or salts can be used such as magnesium nitrite ($Mg(NO_3)_2$) powder can be dissolved in distilled water to become aqueous solution. Then, a quartz substrate which is immersed in this solution subjected to the proper laser beam. The equation below describes the decomposition of magnesium nitrite under the effect of laser heating to obtain MgO nanoparticles [5, 6].

$$Mg(NO_3)_2 \longrightarrow MgO \downarrow + 2NO_2 + ½ O_2$$

In previous studies of the preparation of the nanomaterial, it is observed that the concentration of the solution is very important in getting different sizes of nanoparticles [7]. The laser in this process is considered a heat source and this heat is absorbed by an applicable substrate and through this, the nanomaterial is deposited [8].

The use of the laser differs from the use of the furnace, or other heat sources. The differences lie in the directivity of the laser and its focus on a small area which enable localized deposition in diversity of applicable material [9]. Moreover, the process is faster and more refined in addition to the fact that the used equipments are less compared to those used with other thermal sources [10]. In laser pyrolysis process, the reaction between the laser beam and quartz substrate is limited and the space is very small and it is non-existent with the surrounding media, as a result, the deposition process of impurities is reduced by a high rate [11, 12]. In 2017, Bourrioux and his group prepared nanocomposite ($ZnFe_2O_4/\gamma$-Fe_2O_3) by laser pyrolysis, as this method is characterized by flexibility and multi-use. Then they conducted tests for the nanopowder, and it was found that there are two phases. The bimodal size distribution of small nanoparticles (1-90 nm) and very large particles above 500 nm was detected by SEM and TEM [13]. In 2018, Azhdast and his group conducted a research in the study of laser writing to deposit nanoparticles on the substrate, such as the use of interconnection. They deposited aluminum and copper nanoparticles by laser on a silicon substrate. They also controlled the properties of the particles by determining the laser energy and the number of laser pulses in addition to the interference

of pulses, where this technique is considered the most important alternative to direct writing of lithographic processes to obtain high accuracy [14]. Some recent publications has been reported for deposition nanoparticles by thermal pyrolysis or laser pyrolysis. In 2020, Peter and his group produced silver and gold nanoparticles with titanium dioxide through a process called thermal decomposition, where these nanoparticles were used in nanomedicine and electrochemical devices [15].

In early 2021, Ahmed and his group applied the noble metal nanodots to plasmonic devices after they were manufactured by laser-induced dot transfer technology, and they fixed the compatible gold nanodots on an acceptor substrate with a single laser pulse, of pulse duration in femtoseconds [16]. At the same time, Münevver and his group deposited AgCu nanoparticles by spray pyrolysis, where the size and shape of nanoparticles were studied and characterized by analyzers and imaging devices of the surface [17].

In this work, the laser beam has been utilized to deposit magnesium oxide nanoparticles. The aim of this study is to investigate effects of laser parameters on the deposition features of magnesium oxide nanoparticles on quartz substrate and control the deposition process.

2. Experimental Procedure

Deposition of nanomaterials by laser pyrolysis is an efficient and fast method that provides deposition on quartz substrate. In this work, aqueous solution was obtained by dissolving 1.5g of $MgNO_3$ powder in 10 mL of distilled water. This aqueous solution of MgO_3 has a weak absorbency for the used laser beam compared with high absorption of the substrate. Three Types of lasers were used with different parameters: Q-switched Nd-YAG laser (10ns) pulse duration and variable energy in the range 100 to 1000 mJ, long pulses(0.5ms-5ms) Nd-YAG laser of energy 100 mJ to 10 J and CW CO_2 laser with power in the range 1 to 10 W. Figures 1 and 2 illustrate the experimental setup for both lasers.

High optical quality quartz with dimension (2*2*0.1 cm) was used as a substrate for the deposition process. This type of quartz reduces the absorption effect in the UV-Visible range and optimizes it in theinfrared region where the two employed lasers operate. The quartz substrate was immersed in $MgNO_3$ aqueous solution which is put in a plastic container and then, the laser radiation was directed at the center of the quartz substrate. To conduct laser pyrolysis process, the laser beam of a specific energy for Q-switched & long pulse Nd-YAG laser or specific power of CO_2 laser was subjected to the quartz substrate. The deposition of MgO nanoparticles can be distinguished by naked eyes at the laser beam/quartz interaction region.
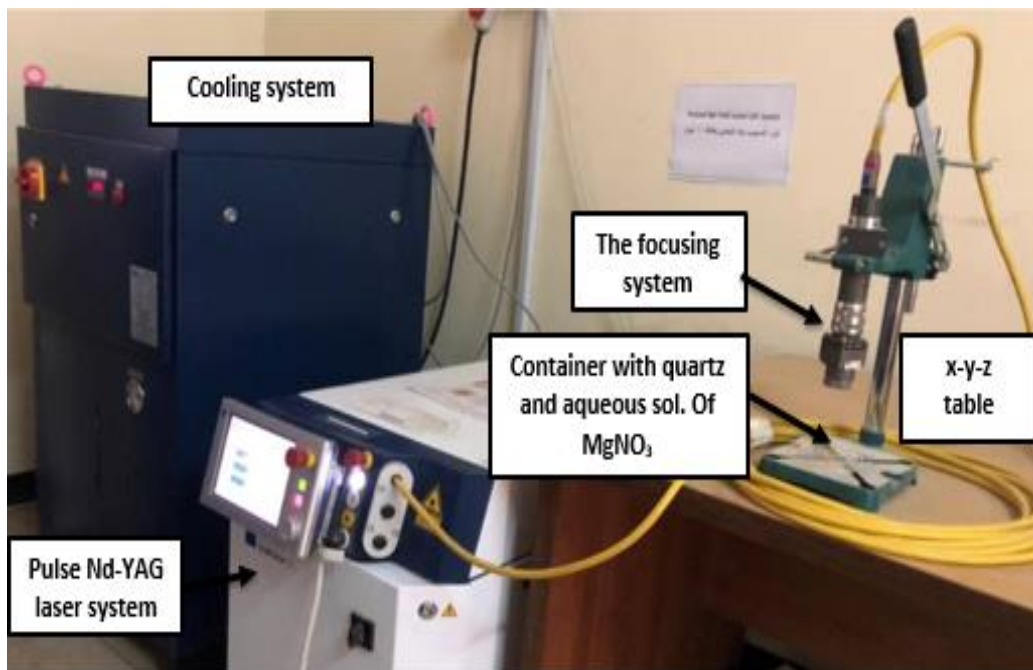
Figure (1): The experimental setup of Nd-YAG laser pyrolysis process.
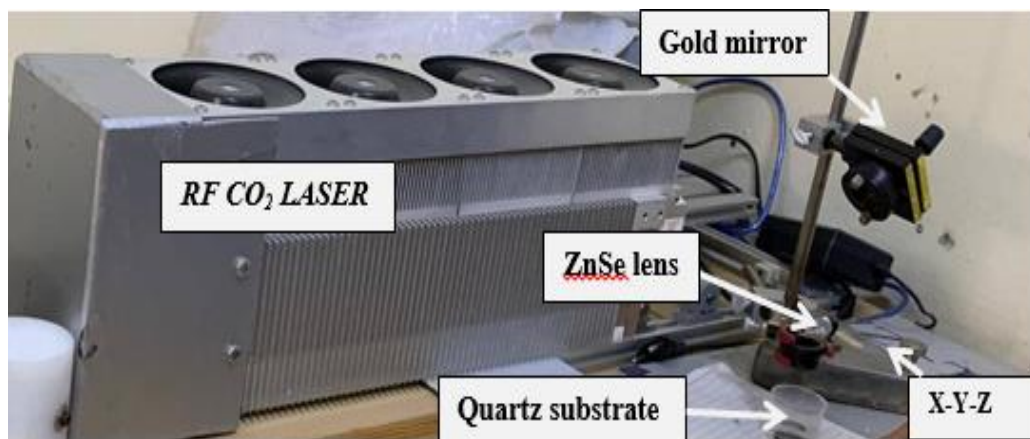
Figure (2): The experimental setup of RF CO₂ laser pyrolysis

3. Results and discussions:

The effect of Nd-YAG laser energy and pulse duration as well as the CO_2 laser power and scanning speed on the deposition process were investigated. Those effects were examined throughout morphological investigation and thermal analyzes.

Various energies were used with Nd-YAG laser (400, 600, 800, 1000) mJ and fixed pulse duration (10 ns) for only one pulse. This parameter has been changed to examine effect on shape and size of MgO nanoparticles and their homogenous distribution.

A. AFM and UV-Visible results

The morphological properties of MgO were examined for different lasers.

1. Short Laser pulses (Nd-YAG laser)

Effect of various laser energies for short laser pulses (Q-switched) Nd-YAG laser was conducted.

Figure (3) shows AFM images of the deposited MgO films and their corresponding size distribution histograms.

Table 1: The average size of MgO nanoparticles and surface Roughness with different laser energies.

Laser energy (mJ)	Avg. Ag Nanoparticles size (nm)	Surface roughness (nm)
400	47.03	18.4
600	41.81	15.6
800	30.29	14.8
1000	24.53	6.97

It is found in that increasing laser energy leads to reduce MgO average size and roughness as given in table 1. A Minimum nanoparticle size of 24.53nm and 6.97nm average size and roughness receptivity were achieved when 1J energy has been used. Figure (4) shows the absorption spectra of MgO nanoparticles prepared by Q-switched Nd-YAG laser with different energies. These spectra reveal appearance of the absorbance at the same wavelength which is attributed to the narrow range of sizes deposited by different laser energies.

a.

b.

c.

d.
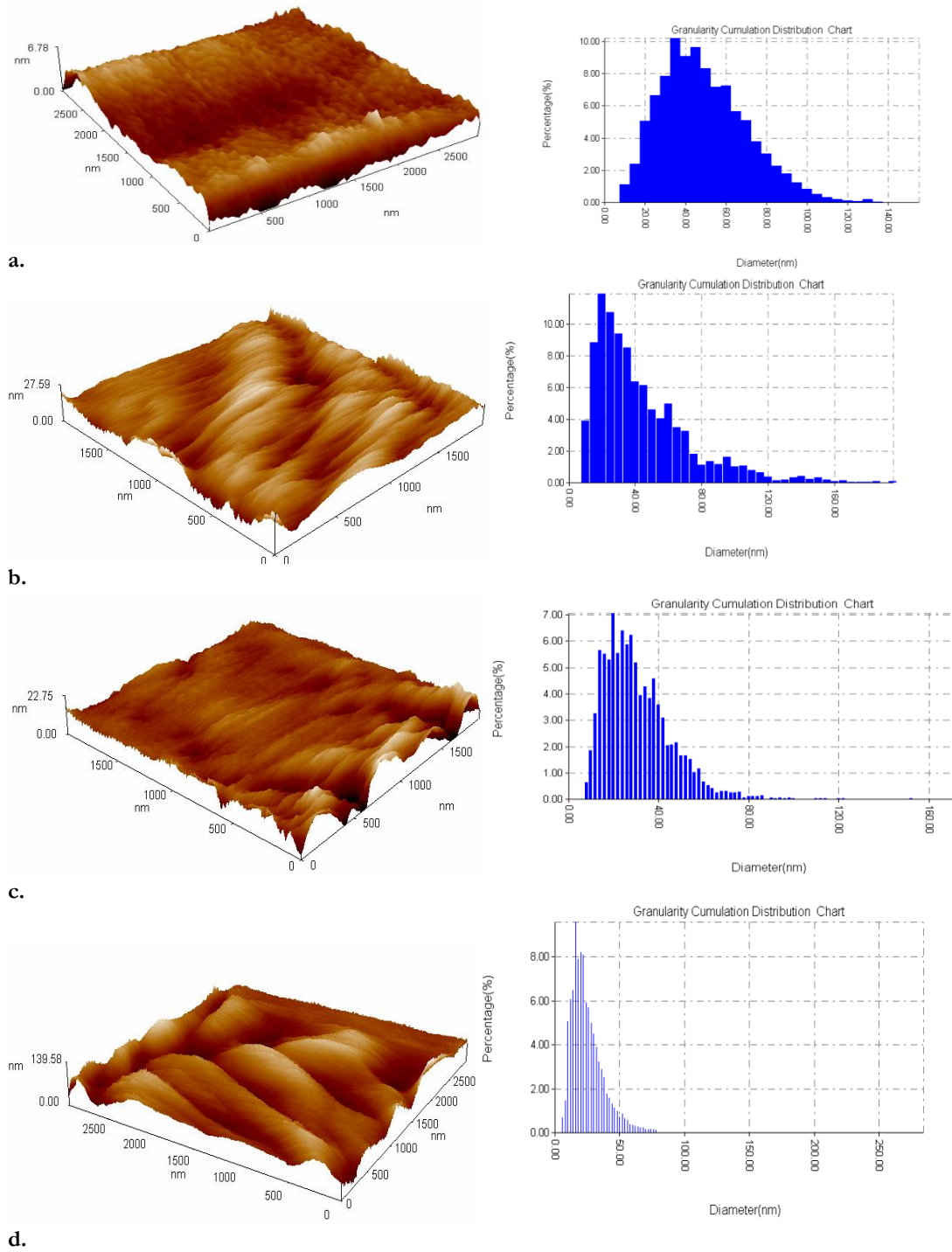
Figure 3: AFM images for Q-switched Nd-YAG laser a)E=400mJ , b)E=600mJ ,c)E=800mj,d)E=1000mJ.
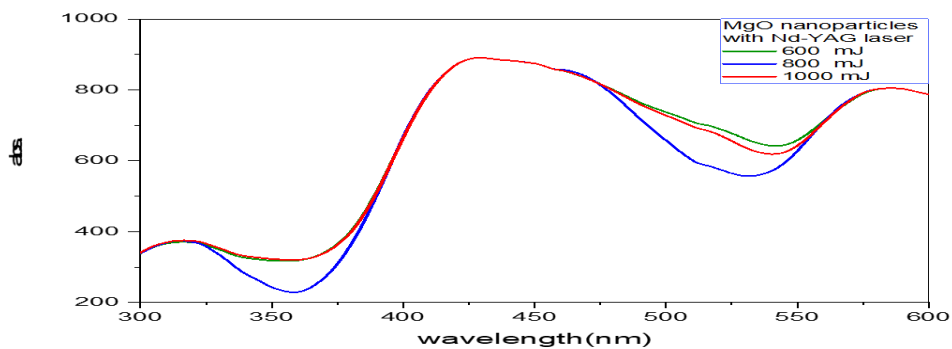
Figure 4: The UV-visible absorbance of MgO nanoparticles deposited by Q-switched Nd-YAG laser.

1. Long Pulse Nd-YAG Laser

Noticeable effect of long laser pulses has distinguished on the surface morphology. AFM images for MgO nanoparticles prepared by pulsed Nd-YAG laser for two different pulse durations with fixed laser energy of 1J is shown in figure 5. The maximum average size was 41.88nm at pulse duration of 1ms as given in Table 2.
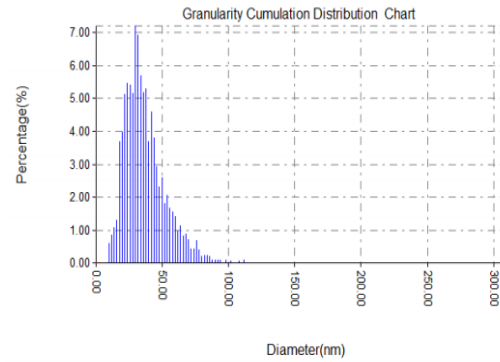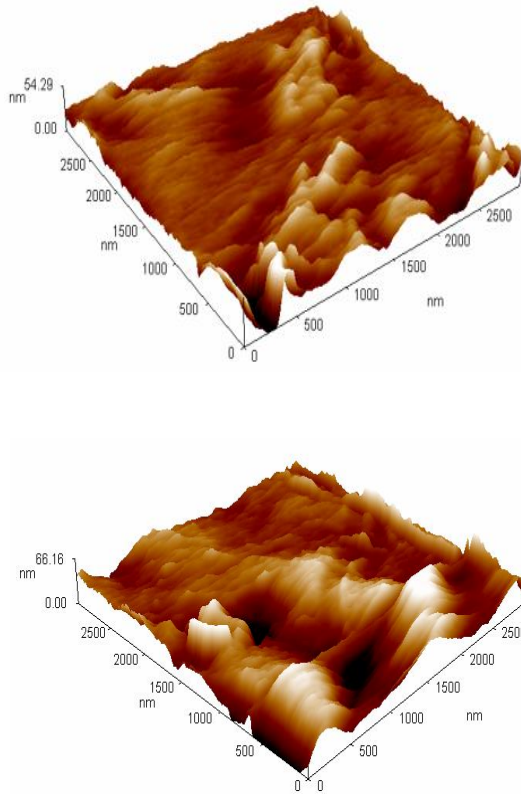
a.
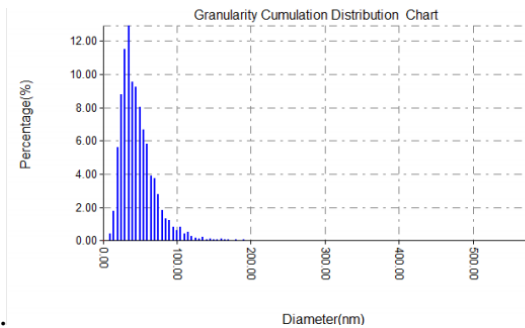
b.

Figure 5: AFM images for Pulsed Nd-YAG laser a) 0.8ms b)1 ms pulse durations.

Table 2: The average size of MgO nanoparticles and surface Roughness with pulse durations

Laser pulse duration (ms)	Avg. size (nm)	Laser roughness (nm)
0.8	37.6	5.13
1	41.88	8.38

The average size of nanoparticles produced by short-pulsed laser at 1 joule and 8 ns, was much smaller than that produced by long pulse laser with the same energy, which is attributed to the high amount of heat which is generated by short laser pulse.

2. RF CW CO_2 Laser

The effect of various RF CO_2 laser scanning speed with fixed power 7W was studied. Figure (6) shows AFM images of MgO nanoparticles produced by different two Scanning speeds.

One can obviously observe that higher temperature produced by lower scanning speed of CO_2 laser is due to strong absorption by the quartz substrate and subsequently, produce smaller MgO nanoparticles as given in Table 3. Similarly, the absorbance spectra for MgO nanofilms have the same peak position at certain wavelength 424nm.

The AFM histograms for the above two mentioned lasers reveal that high number of MgO nanoparticles are located at the laser beam center and is attributed to the Gaussian distribution of the laser intensity. The thermal distribution of laser-quartz interaction will be analyzed later in the next section.

Figure 7 shows that the maximum absorptivity of magnesium oxide nanoparticles was obtained approximately at 420nm for both laser scanning speeds.

Table 3: The average size of MgO nanoparticles and surface roughness with scanning speed.

Scanning speed (mm/s)	Avg. Ag Nps size (nm)	Surface roughness (nm)
0.4	18.8	5.21
1	20.36	7.73
2	23.22	9.32
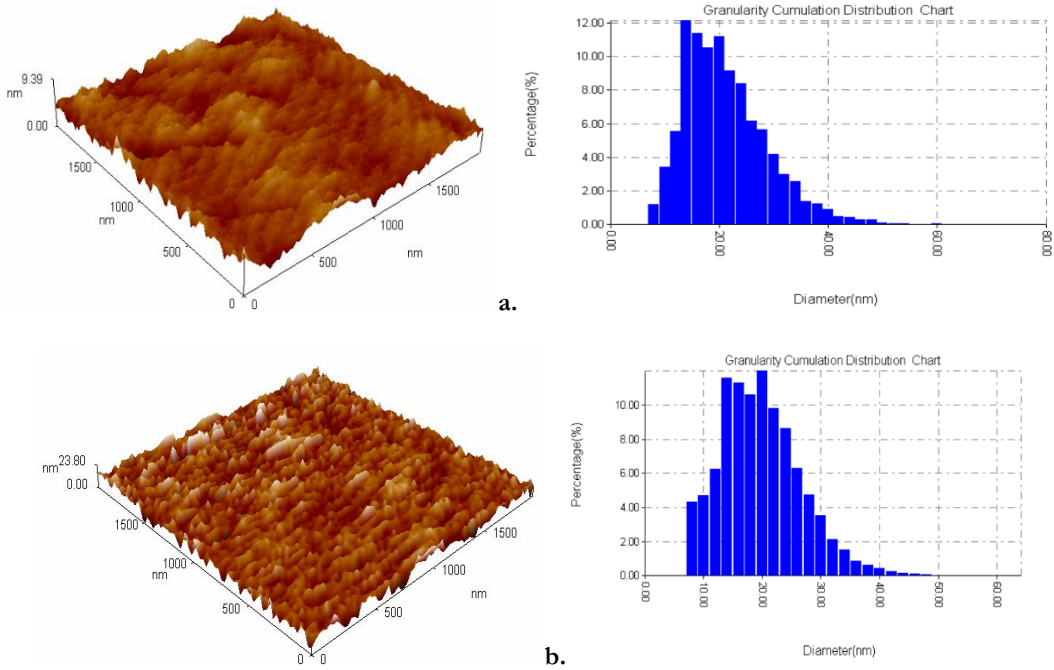
Figure 6: AFM images for RF CO_2 laser a)1mm/s b)0.4 mm/s scanning speed.
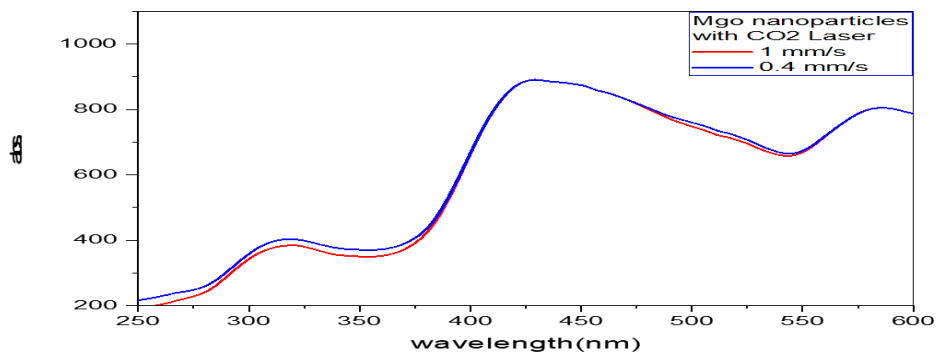
Figure 7: The UV-Visible absorbance of MgO-nanofilm deposited by RF CO_2 laser.

b. Thermal analysis

The thermal analysis for a point heat source (pulse laser) and line source (CW CO_2 laser) were carried out using COMSOL Multiphysics software to find out the generated heat by solving the heat flow theory. It is found that the temperature distribution at the quartz substrate depends on the laser parameters.

This thermal analysis could provide a better understanding about the generated heat at the quartz substrate due to laser absorption. The generated heat is considered as crucial parameter that the deposition process depends on.

1. Short pulse (Q-switched) Nd-YAG Laser

From COMSOL analysis for a point laser model, it was found that when the subjected laser energy on the quartz substrate increased, the temperature increased due to the absorption of Nd-YAG laser energy by the quartz substrate. Table (4) gives the maximum with r=1.5mm obtained at 1 joule, where the temperature reached 440 K, but when r=0.75mm the temperature raised to 1200k for the same laser energy 1 joule.
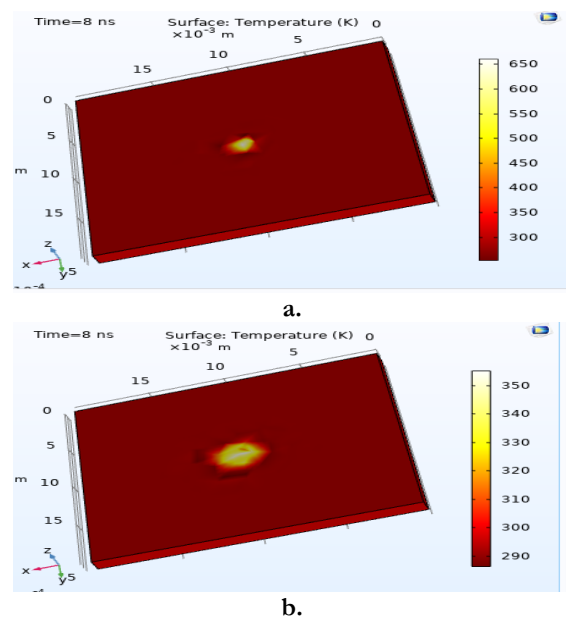
Figure (8): The thermal distribution on the quartz substrate irradiated with short pulse Nd-YAG laser at 400mJ at a) r=0.75mm and b) 1.5 mm beam diameter.

Table (4): Maximum temperature of quartz with different energy irradiated by short pulse laser.

Laser energy (mJ)	Max. Temperature (K) for d=1.5 mm	Max. Temperature (K) for d=7.5 mm
400	350	650
600	380	800
800	400	1000
1000	440	1200

1. RF CO_2 LASER

In this case, one should consider the line source heat flow model for CW CO_2 Laser. When the scanning speed decreased, the temperature increased due to the long time period in which the quartz substrate was exposed to the laser heat. Table (5) gives the maximum temperature at 0.4 mm / s was 850 K.

(a)

(b)

(c)
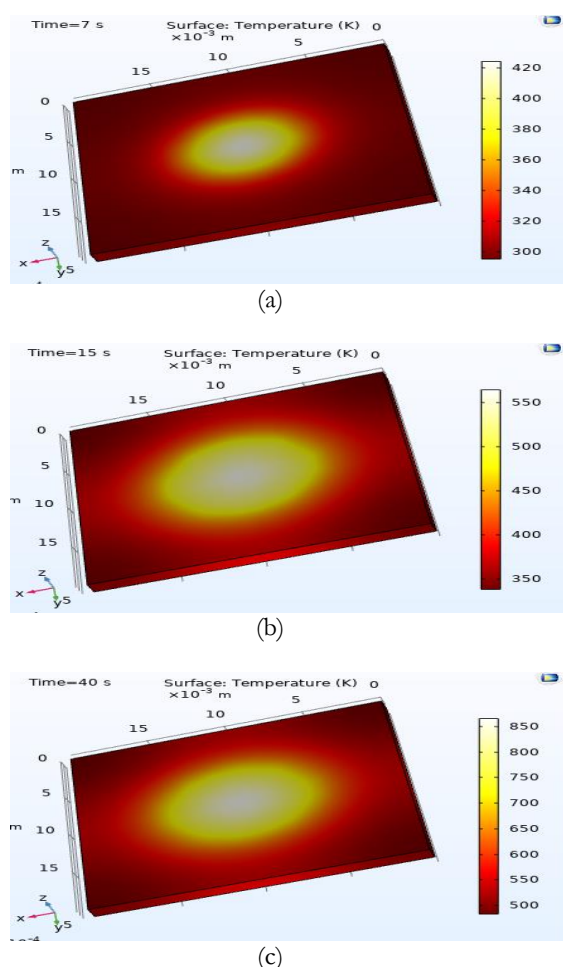
Figure (9): Temperature analysis of quartz substrate irradiated with RF CO_2 Laser for (a)2mm/s, (b)1mm/s, (c)0.4mm/s scanning speed.

Table (5): Maximum temperature on the quartz generated by different scanning speed of RF CO_2 laser.

Laser scan speed (mm/s)	Max. Temperature (K)
0.4	850
1	550
2	420

4. Conclusions:

One can conclude the following remarks extracted from this work. MgO nanoparticles can be deposited by laser pyrolysis using pulse and CW lasers. The deposited nanoparticles form a thin film of a specific roughness which can be controlled by laser parameters. Smaller MgO nanoparticles can be produced using shorter laser pulses (Q-switched) of Nd-YAG laser due to the effect of laser pulse duration. While continuous CO_2 laser is suitable to deposit thick MgO films on a quartz substrate due to the high absorption. The Comsol analysis reveals generation of high temperature at the quartz substrate when a short pulse of Nd-YAG laser or long irradiation CW CO_2 laser. The experimental results are in good agreement with the theoretical model of heat transfer for both point and line source heat flow. The laser beam provides good and accurate control for the generated heat and then the deposited nanoparticle features.

References

[1] V. Sirota, V. Selemenev, M. Kovaleva, I. Pavlenko, K. Mamunin, V. Dokalov and M. Prozorova, "Synthesis of Magnesium Oxide Nanopowder by Thermal Plasma Using Magnesium Nitrate Hexahydrate," Physics Research International, vol. 2016, p. 6853405, 2016.

[2] H. H. H. Hanish, S. J. Edrees and M. M. Shukur, "The Effect of Transition Metals Incorporation on the Structural and Magnetic Properties of Magnesium Oxide Nanoparticles," International Journal of Engineering, vol. 33, no. 4, pp. 647-656, 2020.

[3] L. Shikwambana, M. Govender, B. Mwakikunga, E. Sideras-Haddad and A. Forbes, "A Review of the Laser Pyrolysis Technique Used to Synthesize Vanadium and Tungsten Oxide Thin Films," Advanced Materials Research, vol. 227, pp. 80-83, 2011.

[4] M. Sharma, P. Easha, G. Tapasvi and R. Reetika, "Nanomaterials in biomedical diagnosis," in Nanomaterials in Diagnostic Tools and Devices, Elsevier Inc., 2020, pp. 57-83.

[5] K. H. Stern, "High Temperature Properties and Decomposition of Inorganic Salts Part 3, Nitrates and Nitrites," Journal of Physical and Chemical Reference Data, vol. 1, no. 3, p. 747, 1972.

[6] D. A. R. K. C. Pingali and S. Deng, "Silver Nanoparticles from Ultrasonic Spray Pyrolysis of Aqueous Silver Nitrate," Aerosol Science and Technology, vol. 39, no. 10, pp. 1010-1014, 2005.

[7] A. M. Noori, "Preparation of Ag nanoparticles via pulsed laser ablation in liquid for biological applications," Iraqi Journal of Physics, vol. 15, no. 34, pp. 162-170, 2017.

[8] S. I. Rasmagin, V. I. Kryshtob and I. K. Novikov, "Optical Properties of Thulium-Modified Silver

Nanoparticles," Inorganic Materials, vol. 54, pp. 868-872, 2018.

[9] A. M. 2. A. L. 2. R. M. 1. 2. J. L. H. 1. 2. J. S. Gema Martinez 1 2, "Laser-Assisted Production of Carbon-Encapsulated Pt-Co Alloy Nanoparticles for Preferential Oxidation of Carbon Monoxide," Frontiers in Chemistry, vol. 6, p. 487, 2018.

[10] K. Elihn, F. Otten, M. Boman, P. Heszler, F. Kruis, H. Fissan and J.-O. Carlsson, "Size distributions and synthesis of nanoparticles by photolytic dissociation of ferrocene," Applied Physics A, vol. 72, pp. 29-34, 2001.

[11] E. A. Ganash, G. A. Al-Jabarti and R. M. Altuwirqi, "The synthesis of carbon-based nanomaterials by pulsed laser ablation in water," Materials Research Express, vol. 7, no. 1, p. 015002, 2019.

[12] I. A. Ershov, L. D. Iskhakova, V. I. Krasovskii, F. O. Milovich, S. I. Rasmagin and V. I. Pustovoi, "Synthesis of Silicon-Carbide Nanoparticles by the Laser Pyrolysis of a Mixture of Monosilane and Acetylene," Semiconductors, no. 11, 2020.

[13] S. Bourrioux, L. P. Wang, Y. Rousseau, P. Simon, A. Habert, Y. Leconte, M. T. Sougrati, L. Stievano, L. Monconduit, Z. J. Xu, M. Srinivasan and A. Pasturel, "Evaluation of electrochemical performances of ZnFe2O4/γ-Fe2O3 nanoparticles prepared by laser pyrolysis," New Journal of Chemistry, vol. 41, no. 17, pp. 9236-9243, 2017.

[14] M. H. Azhdast, H. J. Eichler, K. D. Lang and V. Glaw, "Optimization Parameters for Laser-induced Forward Transfer of Al and Cu on Si-wafer Substrate," Optics and Laser Technology, pp. 228-231, 2018.

[15] P. Majerič and R. Rudolf, "Advances in Ultrasonic Spray Pyrolysis Processing of Noble Metal Nanoparticles-Review," Materials (Basel, Switzerland), vol. 13, no. 16, p. 3485, 2020.

[16] Y. Nakata, K. Tsubakimoto, N. Miyanaga, A. Narazaki, T. Shoji and Y. Tsuboi, "Laser-Induced Transfer of Noble Metal Nanodots with Femtosecond Laser-Interference Processing," Nanomaterials, vol. 11, no. 2, p. 305, 2021.

[17] M. Köroğlu, B. Ebin, S. Stopic, S. Gürmen and B. Friedrich, "One Step Production of Silver-Copper (AgCu) Nanoparticles," Metals, vol. 11, no. 9, p. 1466, 2021.